UC Santa Barbara
UC Santa Barbara Previously Published Works

Title

Single-chip wavelength conversion using a photocurrent-driven EAM integrated with a widely tunable sampled-grating DBR laser

Permalink

https://escholarship.org/uc/item/4q0206q9

Journal

IEEE Photonics Technology Letters, 16(9)

ISSN

1041-1135

Authors

Sysak, Matthew N
Barton, J S
Johansson, L A
et al.

Publication Date

2004-09-01

Peer reviewed

Single-Chip Wavelength Conversion Using a Photocurrent-Driven EAM Integrated With a Widely Tunable Sampled-Grating DBR Laser

Matthew N. Sysak, Jonathon S. Barton, *Student Member, IEEE*, Leif A. Johansson, James W. Raring, *Student Member, IEEE*, Erik J. Skogen, *Member, IEEE*, Milan L. Mašanović, *Student Member, IEEE*, Daniel J. Blumenthal, *Fellow, IEEE*, and Larry A. Coldren, *Fellow, IEEE*

Abstract—Tunable photocurrent-driven wavelength converters using widely tunable sampled grating distributed Bragg reflector lasers, electroabsorption modulators, semiconductor optical amplifiers, and an optically preamplified receiver have been fabricated and tested. Dynamic wavelength conversion has been achieved over 40 nm with optical bandwidths up to 10 GHz.

Index Terms—Electroabsorption modulators (EAMs), offset quantum well, sampled grating distributed Bragg reflector (SGDBR) laser, semiconductor lasers, semiconductor optical amplifier (SOA)-PIN receiver, semiconductor optical amplifiers (SOAs), wavelength converters (WCs).

I. INTRODUCTION

NEXT-GENERATION networks using wavelength-division multiplexing will benefit greatly from increased functionality of advanced photonic integrated circuits (PICs). Of particular importance are network functions like wavelength provisioning, add–drop multiplexing, and packet switching that require the use of fast, dynamic wavelength conversion. The InP–InGaAsP offset quantum-well shallow-ridge technology platform has been shown to be convenient for monolithic integration of advanced wavelength agile PICs that promise to perform these functions [1], [2], [4], [6]. Of particular importance are devices that can perform dynamic wavelength conversion. Recently, all-optical wavelength conversion in a Mach–Zehnder interferometer (MZI) monolithically integrated with a widely tunable transmitter [sampled grating distributed Bragg reflector (SGDBR)] has been demonstrated. In this device, no complicated electronics are necessary and it is possible to perform 2R regeneration [tunable all-optical wavelength converter (WC)] [2]. In addition, broad-band, high-speed, field-based, photocurrent-driven (PD) WC designs have been proposed and demonstrated with both MZI and electroabsorption modulators (EAMs) [1], [3]. In this class of WCs, photocurrent from a photodetector is used to modulate the electric field in a reverse biased modulator. Device performance is not limited to carrier modulation effects and inherently
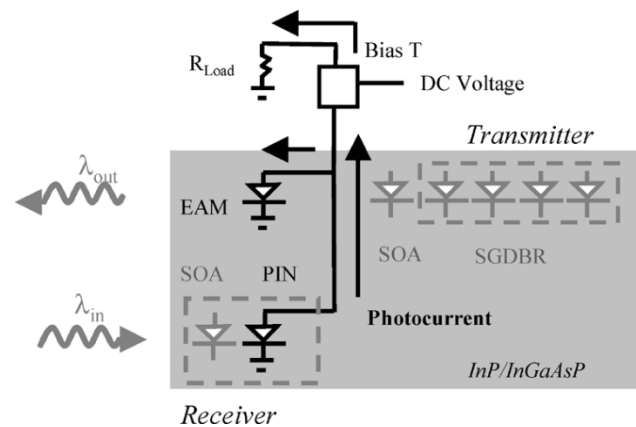
Fig. 1. Diagram of integrated PD-EAM WC with equivalent circuit schematic.

higher modulation bandwidth products are possible. PD-EAM devices traveling-wave EAM/unitraveling-carrier photodiode have been shown to support data rates up to 320 Gb/s [5].

In this work, a widely tunable SGDBR laser has been monolithically integrated with a Franz–Keldysh (FK) EAM, semiconductor optical (SOA) amplifiers, and an FK waveguide photodetector in a PD-EAM arrangement. This design allows for broadband wavelength conversion using high-speed field-based modulation with no required off-chip control wavelength source, no electrical amplification, and no complex optical filtering of output data signals.

II. WAVELENGTH CONVERTER DESIGN

The WC architecture consists of two neighboring ridges interconnected with a gold trace or wirebond. A basic device schematic is shown in Fig. 1. The transmitter ridge consists of an SGDBR laser integrated with a 300-μm-long SOA and an EAM [6]. The receiver ridge contains an input optical preamplifier and an FK-EAM used as a photodetector. The device fabrication process is similar to other SGDBR-based PICs [1], [2], [4], [6] and the final epilayer structure is shown in [1]. For the modulator and detector, a low K dielectric, photo-bis-benzocyclobutene is employed to reduce parasitic pad capacitance. The output and input waveguides are angled to reduce the antireflection coating requirements. Devices have been thinned, and individual bars mounted on aluminum nitride carriers and wirebonded for characterization.
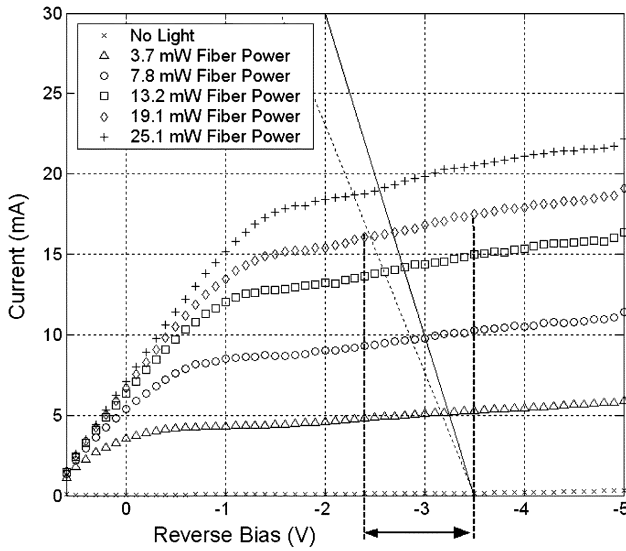
Fig. 2. 200-μm photodetector characteristics as a function of input fiber power. 65- (dotted lines) and 50- (solid lines) Ω load lines shown at -3.5-V bias. Note >1-V swing with 19-mW fiber power using a 65-Ω load.

Fig. 3. DC extinction results for 400-μm FK EAM. Note $\sim$6-dB extinction change with 1-V swing (see Fig. 2) at -3.5-V bias.

III. OPTICAL RECEIVER

It is well known that including an optical preamplifier into integrated optical receiver architectures greatly improves performance by providing optical gain. In the receiver section a broad-band high-saturation power [7] 200-μm-long FK PIN photodiode has been integrated with a 300-μm-long SOA preamplifier similar to that described in [4]. The amplifier provides between 4 and 5 dB of gain and shows 1 dB of gain compression at 10.4-mW input fiber power with 100-mA bias. The compression point is rather high and may be a result of reduced differential gain due to heating. It is important to note that 10.4 mW does not necessarily represent a maximum level of input power to the receiver. It is only for input powers *significantly* above the 1-dB compression point (above $\sim$20 mW) that diminished increases in photocurrent *swing* can be seen as a result of comparative rolloffs in the optical gain between the input signal "1" and "0" level.

IV. DEVICE BIAS AND OPERATION

Due to the complexity of integrating the individual components, care must be taken to select optimum operating conditions. Electrically, the WC consists of two reverse biased diodes (photodetector and EAM) connected to a common DC reverse bias and terminated with a load resistor through a bias-T (Fig. 1). As an example of device operation, load lines (50 and 65 Ω) have been added to show the peak-to-peak voltage swing at a given fiber power level (Fig. 2). This voltage is then translated into a change in extinction in the EAM ($\sim$6 dB for about 1 V, Fig. 3). Generally, it is advantageous to bias the modulator at higher voltages since both the bandwidth (Fig. 4) and slope efficiency is greater. However, operation in this regime increases insertion loss. From Figs. 2 and 3, it is clear that most of the input light is absorbed in the PIN at voltages greater than -2 V and that >10 dB of attenuation of light input into the EAM is also expected. As a result, when the signal photocurrent from the
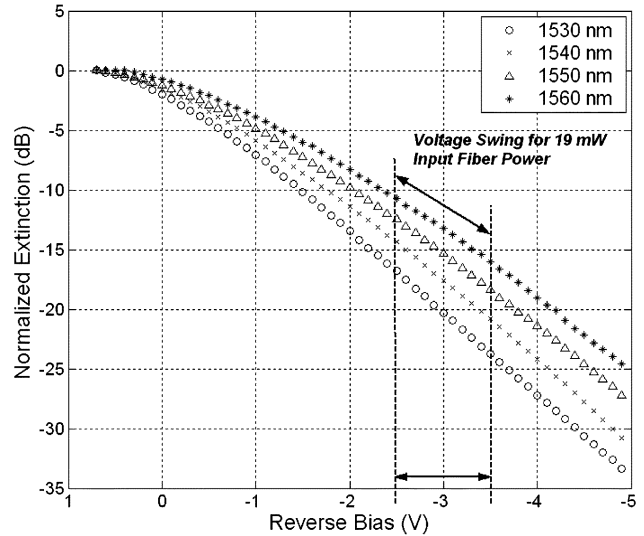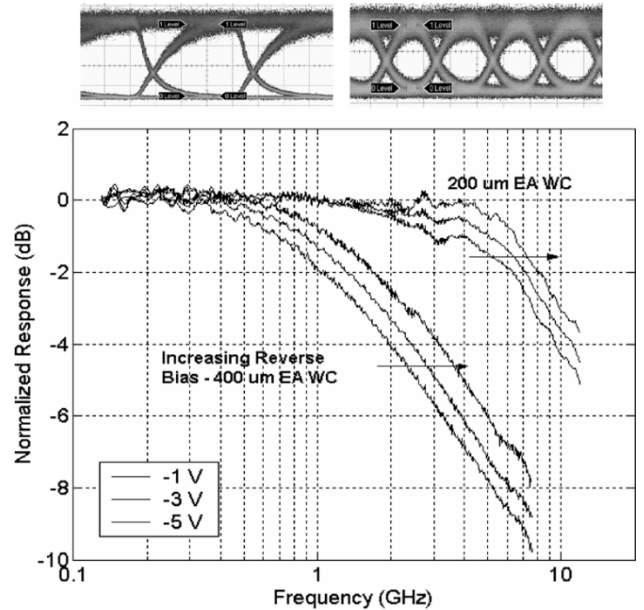

Fig. 4. Optical bandwidth for 75-Ω terminated WC with 400-μm EAM (left) and 50-Ω terminated WC with 200-μm EAM (right) at various reverse bias with 5 mW of input fiber power. Optical eyes at 2.5 (left) and 10 Gb/s (right) are shown above for input power levels of 19.2 mW. Extinction ratios are 14 and 5 dB, respectively, with the limited ER at 10 Gb/s and the slow rise time of the 2.5-Gb/s signal mainly due to the frequency response rolloff.

PIN swings the voltage over the EAM, very little parasitic photocurrent swing is generated that would compete with the PIN signal. This allows the bias point of the entire device beyond -2 V to be selected based on desired EAM efficiency, bandwidth, and output power.

V. EXPERIMENT

Optical bandwidth measurements and bit-error-rate (BER) curves with eye diagrams have been generated. Optical bandwidth measurements were performed using a lightwave optical component analyzer as a function of reverse bias on the device. Light at λ_1 is input from a lensed fiber into the receiver section
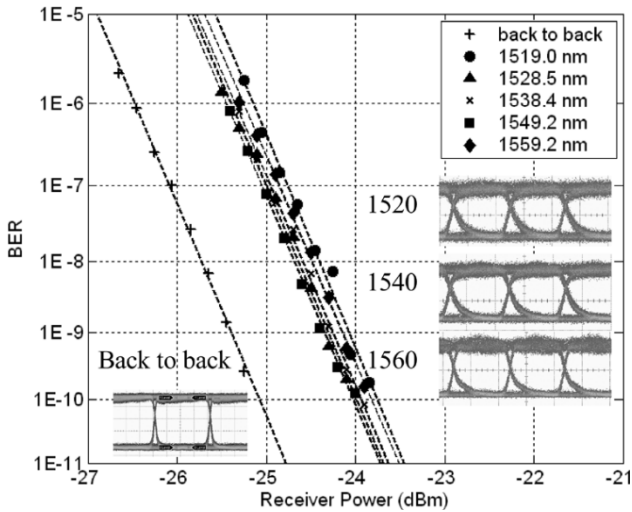
Fig. 5. BER Curves for wavelength conversion. Input wavelength is 1548.1 nm. Eye diagrams are shown for back-to-back operation and conversion to 1520, 1540, and 1560 nm.

of the WC and the output from the transmitter ridge at λ_2 is fed back into a high-speed detector. For the BER measurements, a nonreturn-to-zero $2^{31} - 1$ pseudorandom bit stream at 2.5 Gb/s from a 10-Gb/s BER tester transmitter (Agilent 83 433A) at a wavelength of 1548.1 nm was input into a high-power Erbium-doped fiber amplifier followed by a polarization controller and transmitted to the device under test using a conically tipped lensed fiber. In this experiment, 19.2 mW of optical fiber power was used and the extinction ratio of the input signal was 14 dB. The output optical signal of the WC was then input into a variable optical attenuator before entering the PIN receiver. Note that no output filtering or amplification was required. The BER testing schematic is similar to that in [1]. The laser gain section, preamplifier SOA, and transmitter SOA are biased at 160, 120, and 100 mA, respectively, and the device was maintained at 16 °C with a thermoelectric cooler.

VI. RESULTS

Three separate devices under slightly different conditions have been examined. Optical bandwidth of a 75-Ω terminated 400-μm-long EAM integrated with a 200-μm detector/tunable laser/optical amplifier shows a small signal 3-dB rolloff frequency response of between 2–3 GHz. For a 200-μm-long EAM integrated with a 200-μm passive detector/tunable laser/optical amplifier configuration terminated at 50 Ω, the bandwidth can be extended to 10 GHz (Fig. 4). Small signal circuit models show agreement with experimental results taking into account wirebond inductance from the connection between the chip and carrier.

BER results at 2.5 Gb/s for wavelength conversion are shown in Fig. 5 for the 400-μm-based electroabsorption WC that has been terminated with a 65-Ω load resistor. The device operating point was chosen to maximize output power levels while targeting acceptable system performance and input power requirements. Output waveforms correspond to an extinction ratio of

between 8–8.5 dB over output wavelengths spanning 40 nm with peak output power levels increasing from −7 dBm at 1519 nm to −2.6 dBm at 1559.2 nm. Error-free operation has been achieved with a power penalty of less than 1.5 dB and is in good agreement with expected dispersion penalties given this extinction ratio.

It is possible to improve many of the device characteristics such as extinction ratio, output power, and bandwidth. Higher saturation power preamplifiers will significantly increase the photocurrent generated in the receiver and the voltage drop across the EAM. In addition, narrowing exposed ridge width will provide lower junction capacitance and decrease the resistance–capacitance time constant that limits device bandwidth. Additional approaches for device improvements include increasing the reverse bias, increasing the load resistance, and increasing the EAM length for increased efficiency and extinction ratio.

Optical transmission over 25 and 50 km of fiber at 2.5 Gb/s has also been performed. No noticeable power penalty was observed which is to be expected with a low-chirp FK-based device at these transmission distances [6].

VII. CONCLUSION

We have demonstrated wavelength conversion over a wide wavelength range with optical bandwidths up to 10 GHz. At 2.5 Gb/s, less than 1.5-dB power penalty has been observed with a 65-Ω terminated device that includes a 400-μm-long EAM. In addition, the integrated optical on-chip preamplifier has been shown to provide gain, reducing the fiber power drive requirements considerably from previously reported devices on a similar material platform [1].

REFERENCES

[1] J. S. Barton, E. J. Skogen, M. L. Masanovic, M. N. Sysak, D. J. Blumenthal, and L. A. Coldren, "2.5-Gb/s error-free wavelength conversion using a monolithically-integrated widely-tunable SGDBR-SOA-MZ transmitter and integrated photodetector," *IEEE Photon. Technol. Lett.*, vol. 16, pp. 1531–1533, June 2004.

[2] M. L. Mašanović, V. Lal, J. S. Barton, E. J. Skogen, L. A. Coldren, and D. J. Blumenthal, "Monolithically integrated Mach–Zehnder interferometer wavelength converter and widely-tunable laser in InP," *IEEE Photon. Technol. Lett.*, vol. 15, pp. 1117–1119, Aug. 2003.

[3] H. V. Demir, V. A. Sanabis, O. Fidaner, J. S. Harris Jr., D. A. B. Miller, and J. F. Zheng, "Dual-diode quantum-well modulator for C-band wavelength conversion and broadcasting," *OSA Opt. Express*, vol. 12, no. 2, pp. 310–316, 2004.

[4] B. Mason, J. Barton, G. Fish, and L. Coldren, "Design of sampled grating DBR lasers with integrated semiconductor optical amplifiers," *IEEE Photon. Technol. Lett.*, vol. 12, pp. 762–764, July 2000.

[5] S. Kodama, T. Yoshimatsu, and H. Ito, "320 Gbit/s optical gate monolithically integrating photodiode and electroabsorption modulator," *Electron. Lett.*, vol. 39, no. 4, pp. 383–385, Feb. 2003.

[6] Y. A. Akulova, G. A. Fish, P. C. Koh, C. Schow, P. Kozodoy, A. Dahl, S. Nakagawa, M. Larsen, M. Mack, T. Strand, C. Coldren, E. Hegblom, S. Penniman, T. Wipiejewski, and L. A. Coldren, "Widely tunable electroabsorption-modulated sampled grating DBR laser transmitter," *IEEE J. Select. Topics Quantum Electron.*, vol. 8, pp. 1349–1357, Nov./Dec. 2002.

[7] L. A. Johansson, Y. A. Akulova, G. A. Fish, and L. A. Coldren, "High optical power electroabsorption waveguide modulator," *Electron. Lett.*, vol. 39, no. 4, pp. 364–365, Feb. 2003.